Available online at www.sciencedirect.com
ScienceDirect
Journal of Molecular Catalysis A: Chemical 279 (2008) 1–9
JOURNAL OF MOLECULAR CATALYSIS A: CHEMICAL
www.elsevier.com/locate/molcata

Preferential oxidation of carbon monoxide on CoO_x/ZrO_2

Matthew M. Yung, Zhongkui Zhao, Matthew P. Woods, Umit S. Ozkan *

140W. 19th Avenue, Department of Chemical and Biomolecular Engineering, The Ohio State University, Columbus, OH 43210, USA

Received 19 August 2007; accepted 27 September 2007
Available online 2 October 2007

Abstract

The preferential oxidation (PROX) of carbon monoxide to carbon dioxide in excess H_2 is one of the strategies for obtaining high purity H_2 streams, especially for PEM fuel cells. A CoO_x/ZrO_2 catalyst was synthesized and studied for the PROX reaction under various reaction conditions and indicated that in the temperature window of interest (80–200 °C), this catalyst had potential for obtaining high conversions of CO with high O_2 selectivity to CO_2. Increases in the GHSV and the CO/O_2 ratio led to lower CO conversion but higher O_2 selectivity to CO_2. High temperature operation led to a decrease in CO oxidation activity and the formation of methane, which was attributed to partial reduction of CoO_x/ZrO_2. The catalyst performance was examined using steady-state and transient temperature-programmed reaction (TPRxn) experiments. Temperature-programmed reduction (TPR) and time-on-stream studies were used to examine the catalyst stability in reducing conditions. DRIFTS studies during CO TPD and *in situ* PROX were used to examine surface species on ZrO_2 and CoO_x/ZrO_2.

Keywords: PROX; CO oxidation; Cobalt; ZrO_2; Cobalt oxide; Co/ZrO_2; Co_3O_4

1. Introduction

Proton exchange membrane (PEM) fuel cells have recently garnered much research attention for mobile energy applications due to several factors, including their potential for high efficiency and environmentally friendly operation [1,2]. The electrocatalysts used in hydrogen-powered PEM fuel cells on the anode side, however, require high purity hydrogen streams and can be poisoned by trace amounts of carbon monoxide [3–8]. Hydrogen production from hydrocarbon sources such as coal and natural gas may include steam reforming followed by high and low temperature water gas shift reactors. These streams, however, may still contain a substantial level of CO (0.2–2%) which must be further reduced to ∼10–100 ppm in order to avoid poisoning of the fuel cell catalysts [8–11]. Purification of H_2 streams can be achieved by methods such as pressure-swing adsorption, Pd membrane separation, catalytic methanation, and catalytic preferential oxidation (PROX) of CO. Of these methods, PROX is a possible solution and offers the potential for the lowest cost and ease of implementation, without the parasitic loss of H_2 which occurs during catalytic methanation [2,8].

In the PROX reaction, high activity and selectivity in the same temperature window are essential. For on-board applications, the desired operating temperature should ideally lie between the exit temperature of a low temperature water gas shift reactor (200–250 °C) and operating temperature of a PEM fuel cell (∼80 °C) [12]. Scheme 1 shows the network of the important reactions that should be monitored during PROX studies. The oxidation of CO to CO_2 is the desired route, while the H_2 combustion reaction is the key undesired competitive reaction, especially at higher temperatures. While methanation eliminates CO, it does so at the expense of H_2. The Boudouard reaction also eliminates CO, but the deposition of coke is well known to decrease catalytic activity, so this reaction should be avoided. Water gas shift activity would also help eliminate CO and produce additional H_2.

In addition to the wealth of literature on CO oxidation, much work has been conducted on the PROX reaction. Early work on PROX by Oh and Sinkevitch investigated several noble metals supported on alumina as well as various transition metal based catalyst compositions and platinum was found to be among the best candidate materials [13]. Noble metal catalysts, especially platinum and gold, have been among the most studied systems [14–22]. Platinum has generally been considered to be more active, while gold catalysts provide higher O_2 selectivity to CO_2 [14]. Some studies have also

* Corresponding author. Tel.: +1 614 292 6623; fax: +1 614 292 3769.
E-mail address: ozkan.1@osu.edu (U.S. Ozkan).

1381-1169/$ – see front matter © 2007 Elsevier B.V. All rights reserved.
doi:10.1016/j.molcata.2007.09.026

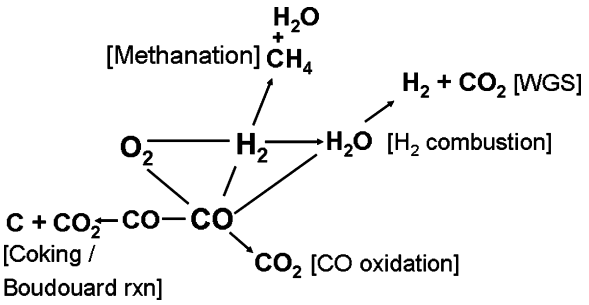

Scheme 1. Diagram of key reactions in the PROX network.

examined lower cost transition metals for the PROX reaction.

Mechanistic studies on CO oxidation in excess O_2 were carried out and showed cobalt to be an active metal for the reaction, though carbonate formation could lead to decreased activity at temperatures below 100 °C [23]. Other studies have shown strong promotional effects of Co and Fe to Pt/Al_2O_3 catalysts, leading to substantial activity gains for the PROX reaction [24–27]. Studies without Pt, using solely Co, indicate that Co_3O_4 is active for CO oxidation but that bulk cobalt oxide may reduce to metallic Co^0 under an excess H_2 atmosphere [28,29]. These studies indicate that a highly oxidized form of cobalt that exhibits strong interaction with a defect-forming support and allows CO activation could lead to high activity for the preferential oxidation of CO in excess H_2.

Additional studies for PROX on bulk transition metal oxides found that operation at high temperatures could lead to a reduction to lower valency oxides or to metallic phases, which could in turn lead to increased activity for H_2 combustion and methane formation. Of the metal oxides that were tested, cobalt oxide was the most active and also showed high selectivity over a broad temperature window [30]. To further examine CoO_x-based catalysts, a series of cobalt catalysts on various metal oxide supports have been prepared in our laboratories. We have found that high CO oxidation activity could be obtained on cobalt-based catalysts [31–33] and that a ZrO_2 support provided higher rates of CO conversion than other metal oxide supports. In the present work, a CoO_x/ZrO_2 catalyst is examined for its activity for the PROX reaction and the influence of GHSV, O_2/CO ratio, and stability in reducing conditions are explored.

2. Experimental

2.1. Catalysts synthesis

The incipient wetness impregnation technique was used to synthesize a catalyst consisting of 10 wt% cobalt on ZrO_2. An aqueous solution of the cobalt nitrate precursor, $Co(NO_3)_2{\cdot}6H_2O$ (Aldrich), was used to impregnate a ZrO_2 support provided by Saint Gobain (Lot 2000920047). Three impregnation steps were performed on the catalyst, with a 4 h drying period between steps in an oven at 110 °C. After the final impregnation, the catalyst was placed in the oven overnight. After drying, the sample was transferred to a calcination furnace and heated at a rate of 10 °C/min to 500 °C in air and held here for 3 h. The catalyst used in this study has been previously characterized by XPS, XRD, TPR, and laser Raman spectroscopy and the results indicated that after calcination, Co_3O_4 formed on the monoclinic ZrO_2 support [32,33].

2.2. Catalyst reaction testing

Activity measurements were performed using a stainless steel tube (1/4 in. O.D.) fixed bed reactor. The reactor furnace was controlled by an Omega CN49000 temperature controller and K-type thermocouple in direct contact with the quartz wool plug upstream of the catalyst bed. All tubing and connections were made of Swagelok stainless steel fittings. Brooks 5850E mass flow controllers were used to control the gas flow rate. The gas hourly space velocity and reactant concentrations were varied among experiments and a GHSV = 39,000 h^{-1}, corresponding to 200 mg catalyst and 50 cm^3(STP)/min, was used for most experiments. The samples were pretreated in 10% O_2 in balance Ar at 300 °C for 30 min before experiments. Analysis of the feed and effluent gas streams was conducted using a HP 5890 gas chromatograph equipped with molecular sieve and Porapak Q separation columns and a TCD and an FID with a methanizer. Activity measurements were taken at 30 and 60 min and averaged. Time-on-stream studies were performed using a Varian 4900 Micro-GC with TCD and Poraplot Q columns and TCD detectors. The conversions of CO (X_{CO}) and O_2 (X_{O_2}) as well as the O_2 selectivity to CO_2 (S_{CO_2}) are defined as follows:

$$X_{CO} = \frac{[CO]_{in} - [CO]_{out}}{[CO]_{in}},$$

$$X_{O_2} = \frac{[O_2]_{in} - [O_2]_{out}}{[O_2]_{in}},$$

and

$$S_{CO_2} = \frac{[CO_2]_{out} - [CO_2]_{in}}{2([O_2]_{in} - [O_2]_{out})}.$$

Temperature-programmed reaction (TPRxn) studies utilized a Cirrus RGA quadrupole mass spectrometer to monitor the reactor effluent. Before the experiment, the sample was pretreated at 300 °C for 30 min in 10% O_2/He, and was then cooled to room temperature under He flow. The total gas flow rate was 30 cm^3(STP)/min and 100 mg of CoO_x/ZrO_2 was loaded into the reactor. The temperature was increased at 5 °C/min from room temperature to 300 °C, and held for 30 min. The feed composition was 1% CO, 1% O_2, 60% H_2, and balance He.

2.3. Catalyst characterization

N_2 physisorption was conducted on a Micromeretics ASAP 2010 at 77 K and the BET surface area of the ZrO_2 was determined to be 48 m^2/g and the CoO_x/ZrO_2 catalyst had a surface area of 41 m^2/g.

Temperature-programmed reduction (TPR) experiments were performed on an in-house constructed system equipped with a TCD detector to measure H_2 consumption. A water trap removed moisture from the TPR effluent stream before

reaching the TCD. Quartz U-tube reactors were loaded with 100 mg of sample and catalysts were pretreated by heating in 20% O_2/N_2 at 300 °C for 30 min and were then cooled to room temperature under N_2 flow. To simulate operation in reducing conditions, additional pretreatments were performed by ramping the sample at 10 °C/min in 100% H_2 and holding at the final temperature (either 100 °C or 200 °C) for 3 h and then cooling to room temperature under N_2 flow. The TPR was performed using 30 cm^3/min of 10% H_2/N_2 and temperature was ramped from 25 °C to 800 °C at 10 °C/min.

Diffuse reflectance infrared Fourier transform spectroscopy (DRIFTS) experiments were performed with a Thermo Nicolet 6700 spectrometer with a KBr beamsplitter and a liquid N_2 cooled MCT detector at a spectral resolution of 4 cm^{-1}. Samples were pretreated at 400 °C in 5% O_2/He for 30 min at a flow rate of 25 mL/min, and backgrounds were taken while cooling under He flow. For the TPD experiments, adsorption of 1% CO in balance He was performed for 30 min at 50 °C and the sample was then flushed with He for 10 min. The sample was heated and held for 10 min at various temperatures from 50 °C to 400 °C while spectra were collected. For the *in situ* reaction experiments, backgrounds were collected in the same fashion as during the CO TPD experiments. The samples were exposed to 25 mL/min of 1% CO, 1% O_2, and 60% H_2 in balance He and spectra were acquired during flow of reactants.

3. Results and discussion

3.1. Effect of GHSV and CO/O_2 ratio on steady-state PROX reaction

The activity of the CoO_x/ZrO_2 catalyst was evaluated at three different gas hourly space velocities: 19,500 h^{-1}; 39,000 h^{-1}; and 78,000 h^{-1}. In these experiments, the feed gas composition was 5000 ppm CO, 5000 ppm O_2, 5% H_2 and balance Ar. The CO conversion and O_2 selectivity to CO_2 during these experiments are displayed in Fig. 1. As expected, increasing the space velocity led to decreases in the CO conversions, as shown in Fig. 1a. The two lower space velocities (19,500 h^{-1} and 39,000 h^{-1}) reached 100% CO conversion at 125 °C. The sample tested at a space velocity of 78,000 h^{-1} achieved complete CO conversion at 150 °C. These results indicate that for the given test conditions, complete CO conversion can be achieved within the desired operating temperature window over a broad range of residence times. The O_2 conversion (not shown) showed the same trend as the CO conversion, namely, decreased conversion with increasing space velocity.

Examining the O_2 selectivity to CO_2 in Fig. 1b shows that the CoO_x/ZrO_2 catalyst was highly selective (>90%) when the temperature was at 125 °C or below. As temperature was raised to 150 °C and higher, a clear drop in selectivity was observed. The high space velocity experiment exhibited the highest selectivity in the 125–200 °C temperature range. An increase in O_2 selectivity to CO_2 with increasing space velocity was observed, which is due to the lesser extent of the hydrogen combustion reaction during the experiments at the higher space velocities.

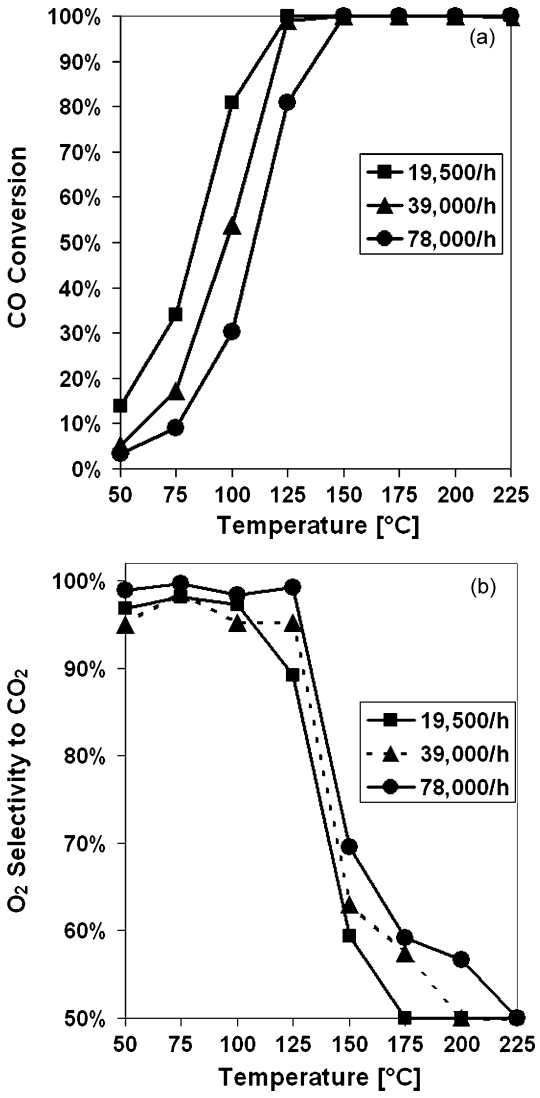

Fig. 1. (a) CO conversion and (b) O_2 selectivity to CO_2 over CoO_x/ZrO_2 at GHSV of (■) 19,500 h^{-1}, (▲) 39,000 h^{-1}, and (●) 78,000 h^{-1} in the presence of 5000 ppm CO, 5000 ppm O_2, 5% H_2, and balance Ar.

The ratio of CO to O_2 is another important variable in the PROX reaction and can alter both the CO conversion and O_2 selectivity to CO_2. A decrease in this ratio typically leads to an increase in CO conversion and a decrease in O_2 selectivity. A stoichiometric ratio of CO and O_2 was tested over the CoO_x/ZrO_2 at two space velocities (39,000 h^{-1} and 78,000 h^{-1}). The reactant concentrations were 5000 ppm CO, 2500 ppm O_2, 5% H_2, and balance Ar. Over an entirely selective catalyst, one would expect the conversion of CO and O_2 to be identical under these stoichiometric reaction conditions. For the space velocity of 39,000 h^{-1} in Fig. 2a, the conversion of CO and O_2 is nearly identical up until 150 °C, corresponding to O_2 selectivity to CO_2 of >95%. At temperatures above 150 °C, the O_2 conversion remains at 100%, while the CO conversion begins to decrease due to competition between the selective oxidation and the hydrogen combustion reaction. In these stoichiometric CO/O_2 experiments, any O_2 that reacts with H_2 results in a shortage in O_2 that is available for reaction with CO. The deviation between the CO and

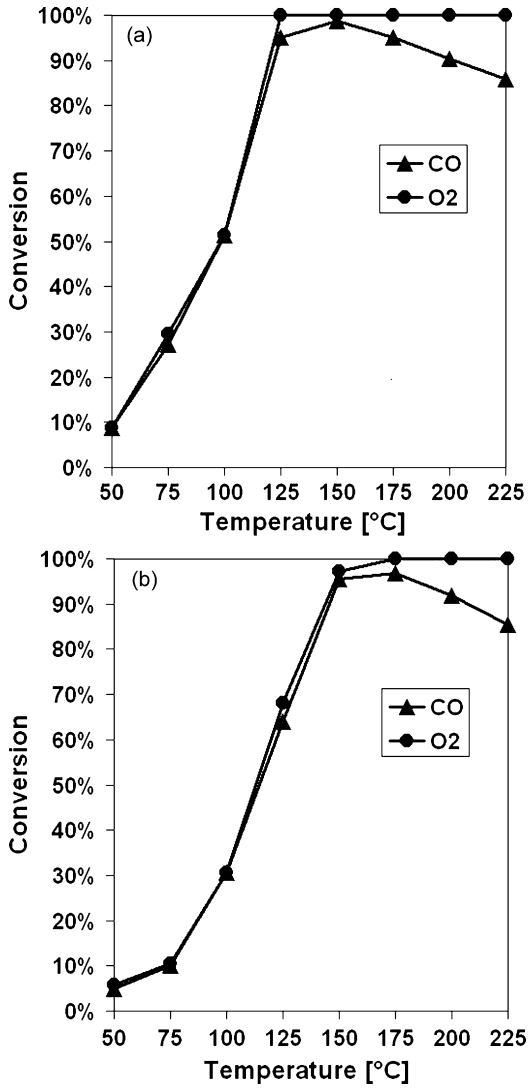

Fig. 2. Conversion of (▲) CO and (●) O_2 over CoO_x/ZrO_2 in the presence of 5000 ppm CO, 2500 ppm O_2, 5% H_2, and balance Ar at GHSV of (a) 39,000 h^{-1} and (b) 78,000 h^{-1}.

O_2 conversions at temperatures of 175 °C and higher shows the increasing significance of the H_2 combustion with elevated temperatures.

The experiment using the stoichiometric CO/O_2 mixture at a space velocity of 78,000 h^{-1} is shown in Fig. 2b. The conversions of CO and O_2 are similar to one another at temperatures of 175 °C and below, again indicating high O_2 selectivity to CO_2 (>95%). In this experiment, the decrease in the CO conversion, resulting from an inadequate supply of O_2, does not occur until the temperature was raised from 175 °C to 200 °C. The comparison of Fig. 2a and b shows that for the 2:1 CO/O_2 molar ratio, at higher temperatures a higher space velocity results in higher O_2 selectivity to CO_2, which corroborates the results in Fig. 1b.

3.2. Temperature-programmed reaction (TPRxn)

In order to obtain additional insight into the PROX reaction and competing reactions over our CoO_x/ZrO_2 catalyst, a temperature-programmed reaction experiment was conducted. The signals for $m/z = 15$ (CH_4), 18 (H_2O), 28 (CO, corrected to account for fragmentation of CO_2), and 44 (CO_2) during this experiment are presented in Fig. 3. By monitoring the CO signal, three distinct regions can be identified. The first region is the highly O_2 selective oxidation of CO to CO_2, which occurs at 175 °C and below. In this region, simultaneous decreases in the intensities of CO and O_2 are mirrored by an increase in the CO_2 signal. The water signal shows only a small deviation from its baseline value. The dominant reaction in this region is CO oxidation. The second region starts when the temperature reaches 175 °C. At 175 °C, a minimum in the CO signal is reached and the O_2 signal falls to a negligible value. At this point, the combination of the CO oxidation and H_2 combustion reactions has essentially depleted oxygen from the system. As the temperature is increased beyond this point, the H_2 combustion reaction becomes more favorable, which can be observed by the decrease in CO conversion. The competition from H_2 combustion can be seen by the sudden increase in the water signal, as well as an increase in CO intensity and simultaneous decrease in the CO_2 signal. At the start of the third region, the CO intensity goes through a maximum around 250 °C and additional temperature increases lead to additional CO conversion. In this region (250–300 °C) the decrease in CO intensity is attributed to the methanation reaction, due to the sharp increase in the CH_4 signal while the CO_2 intensity continues to decrease with increasing temperature. The onset of the methanation reaction could be due to an increased extent of reduction of cobalt oxide on the catalyst surface. The high temperature shoulder on the CO_2 signal could arise from desorption of surface carbonate species as CO_2 or additional CO_2 formation from the combustion of the freshly formed CH_4 in the reactor.

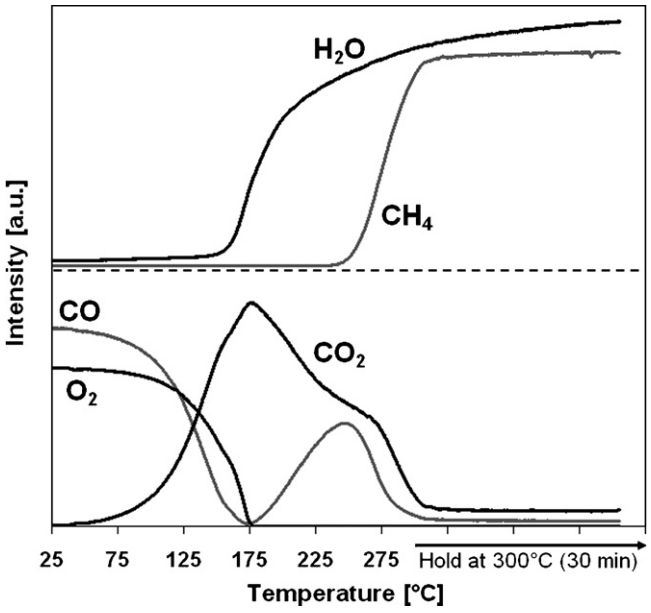

Fig. 3. Temperature-programmed reaction over CoO_x/ZrO_2 in the presence of 1% CO, 1% O_2, 60% H_2, balance He.

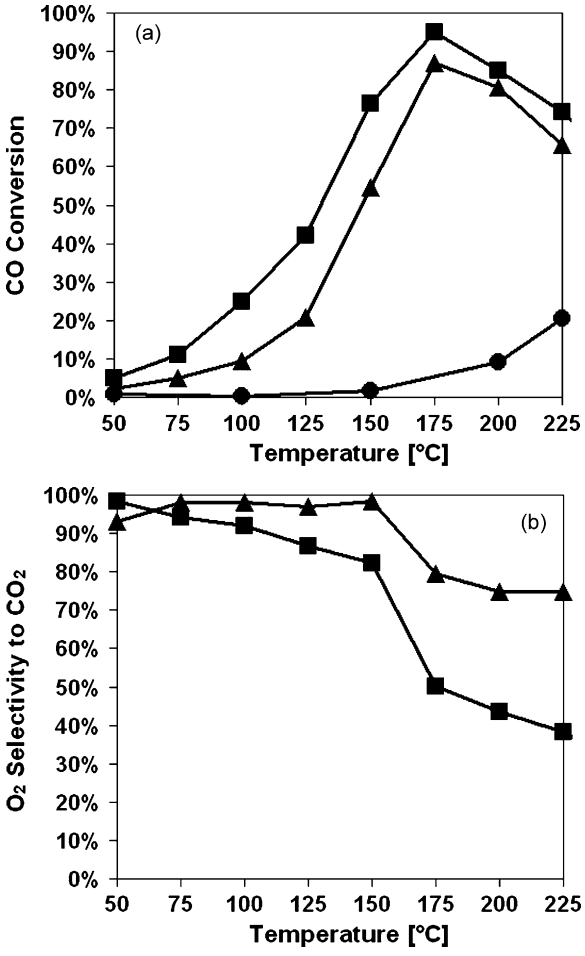

Fig. 4. Effect of CO/O_2 ratio on (a) CO conversion and (b) O_2 selectivity to CO_2 over CoO_x/ZrO_2 at GHSV of 39,000 h^{-1}. (■) 1% CO, 1% O_2, 60% H_2 in Ar. (▲) 1% CO, 0.5% O_2, 60% H_2 in Ar. (●) CO conversion on unloaded ZrO_2 in 1% CO, 1% O_2, 60% H_2 in Ar.

3.3. Activity studies in high H_2 concentrations

Steady-state reaction experiments were performed in order to examine the catalytic activity and effect of the CO-to-O_2 ratio in higher H_2 concentrations for the PROX reaction over CoO_x/ZrO_2. The feed gas composition was 1% CO (0.5% or 1% O_2), and 60% H_2 in balance Ar. The bare ZrO_2 support, without cobalt impregnation, was also tested for the PROX reaction using feed stream with the higher O_2 concentration. In Fig. 4a, a change from excess to stoichiometric oxygen over CoO_x/ZrO_2 showed a slight decrease in the rate of CO conversion for all temperatures. The shape of the CO conversion curve, however, was not affected. In both experiments, the CO conversion rate increases until 175 °C at which point it decreases due to competition with the H_2 combustion reaction. The CO conversion over the bare ZrO_2 was lower than over the CoO_x/ZrO_2 catalyst, reaching only 20% at 225 °C. The bare ZrO_2 support was also more selective for H_2 combustion than CO oxidation, and had O_2 selectivity to $CO_2 < 30\%$. The low CO conversion and O_2 selectivity over ZrO_2 indicate that the presence of cobalt oxide is primarily responsible for the catalytic activity for the CO oxidation reaction. The O_2 selectivities to CO_2 over CoO_x/ZrO_2 during these experiments are presented in Fig. 4b. The O_2 selectivity to CO_2 was higher during the experiment using the lower oxygen concentration. Both ratios of CO/O_2 showed selectivities >80% at temperatures of 150 °C and below. At 175 °C and above, the reaction using the higher oxygen concentration showed a sharp decline in selectivity to <40% while the stoichiometric CO/O_2 reaction exhibited ~75% selectivity at 225 °C.

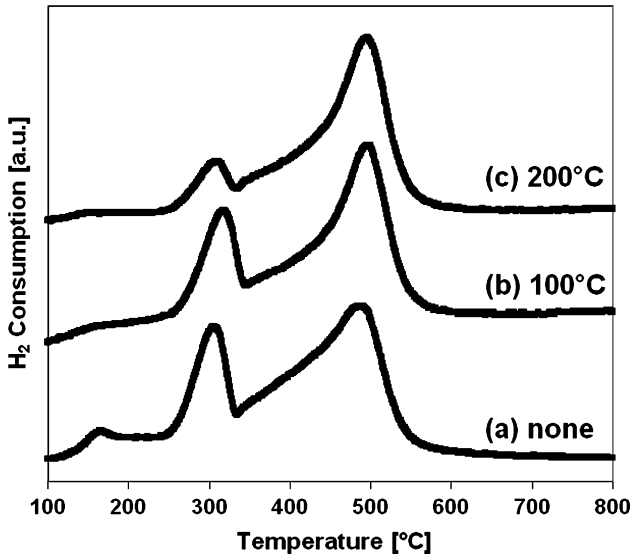

Fig. 5. Temperature-programmed reduction of CoO_x/ZrO_2 in 10% H_2/N_2 after (a) no pretreatment or pretreatment in 100% H_2 for 3 h at (b) 100 °C or (c) 200 °C.

3.4. Catalyst stability in reducing conditions

A commercial PROX catalyst would operate in overall reducing conditions. Temperature-programmed reduction experiments were performed in order to examine the influence of reducing conditions on the catalyst structure and metal-support interactions. Fig. 5 shows the TPR profiles for fresh CoO_x/ZrO_2 and after a 3-h pretreatment in H_2 at two different temperatures. Two distinct reduction features are visible. The reduction features around 300 °C and 500 °C have previously been attributed to the transitions from Co^{3+} to Co^{2+} and Co^{2+} to metallic Co, respectively [32,34–36]. In comparison with the fresh sample, pretreatment at 100 °C had little influence on the TPR profile. The pretreatment in H_2 at 200 °C, however, led to a significant decrease in the low temperature reduction feature as compared to the fresh sample and sample pretreated at 100 °C. The pretreatment at 200 °C that led to a change in the catalyst structure due to a partial reduction indicates that long-term stability could be a concern for high (~200 °C) operating temperatures.

In order to examine the stability of this catalyst in operating conditions, a time-on-stream experiment was conducted. The feed stream consisted of 1% CO, 1% O_2, and 60% H_2 in balance He at 175 °C at GHSV of 19,500 h^{-1}. Fig. 6 shows that at 175 °C, there is an early decline in CO conversion that occurs after which point the activity seems to stabilize. This loss of activity could be due to the reduction of CoO_x to a lower valency [30]. While the activity level appears to have reached a constant level, time-

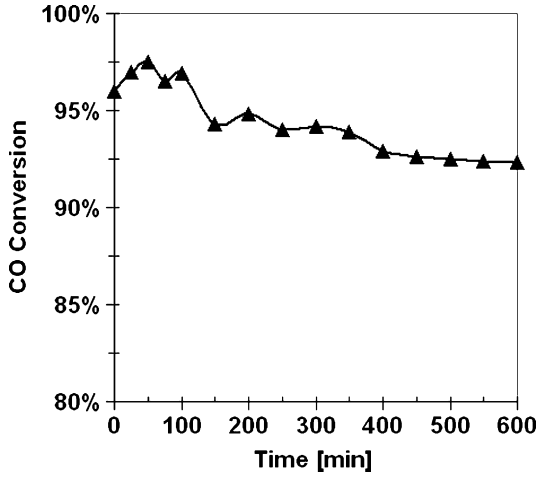

Fig. 6. Time-on-stream CO conversion on CoO_x/ZrO_2 at 175 °C in the presence of 1% CO, 1% O_2, and 60% H_2 in balance He at GHSV of 19,500 h^{-1}.

on-stream studies examining CO conversion over much longer periods should be performed.

3.5. Investigation of surface species using DRIFTS

3.5.1. CO TPD

Following the adsorption of CO and flushing with He, the DRIFT spectra on ZrO_2 and CoO_x/ZrO_2 were obtained at increasing temperatures to examine the types of surface species. For the CO TPD on ZrO_2, the high wavenumber region in Fig. 7a exhibits three distinct negative bands at 3773, 3736, and 3676 cm^{-1} that correspond to terminal, bi-bridged, and tri-bridged OH groups [37], respectively, on ZrO_2 and the broad positive band from 3600 to 3000 cm^{-1} is typical of the OH vibration of physically adsorbed H_2O. A bidentate formate species can be weakly observed by a combination band at 2971 cm^{-1} and the C–H stretch at 2873 cm^{-1} [38]. In the low wavenumber region (Fig. 7b), bidentate formate is observed from the band at 1584 cm^{-1} as well as the C–H bending and symmetric C–O stretching modes at 1379 cm^{-1} and 1358 cm^{-1}, respectively [38]. In similar experiments, it has been observed that following the adsorption of CO, formate species require the presence of surface hydroxyl groups in order to form, which is consistent with the previously mentioned negative hydroxyl bands at 3773, 3737, and 3676 cm^{-1} due to hydroxyl interaction with CO [37,38]. Also in the lower wavenumber region, the band at 1624 cm^{-1} has been assigned to bidentate bicarbonate [39]. Other bands in the 1800–1100 cm^{-1} have been assigned to ionic carbonate at 1456 cm^{-1} which red shifts to 1440 cm^{-1} at 400 °C [38] and carbonate species at 1300 cm^{-1}, 1235 cm^{-1}, and 1198 cm^{-1} [40–42]. As the temperature is raised, the negative hydroxyl bands are nearly completely recovered by 400 °C and broad band due to physisorbed water has disappeared. The bidentate bicarbonate band at 1624 cm^{-1} decreases with increasing temperature and red shifts to 1603 cm^{-1}, becoming a shoulder in the bidentate formate band (which has red shifted to 1570 cm^{-1}). Concurrently, the carbonate band at 1300 cm^{-1} decreases before being undetectable at 200 °C and a band forms

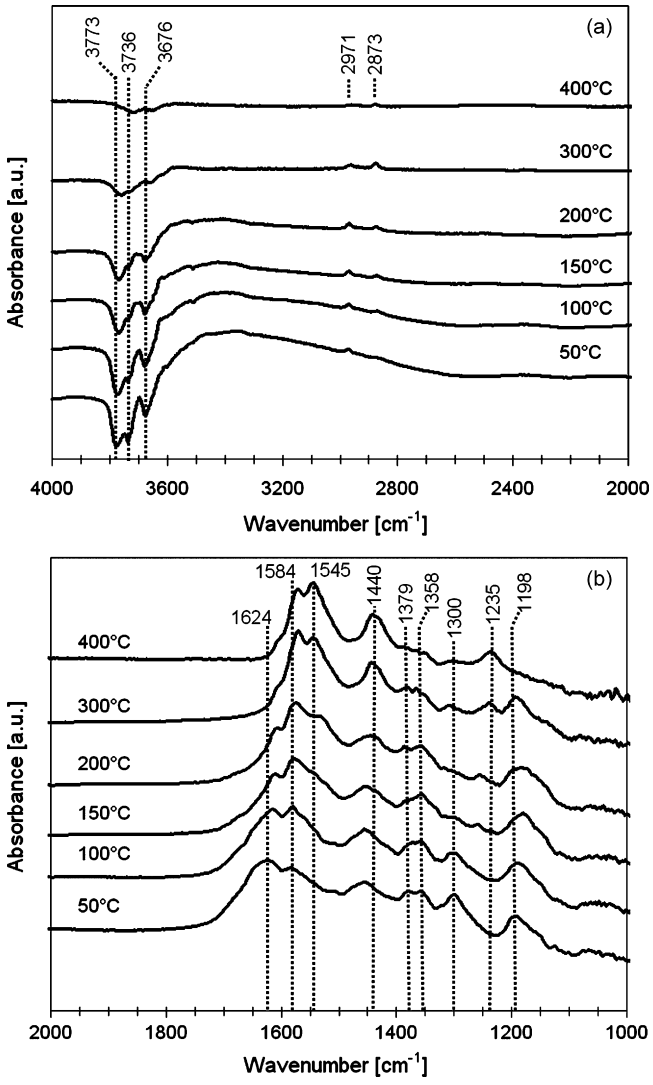

Fig. 7. DRIFTS spectra of ZrO_2 under 25 cm^3/min He following 30 min adsorption of 1% CO, referenced to ZrO_2 under He flow at each temperature.

at 1545 cm^{-1} which has been assigned to surface carbonates [43].

Fig. 8 shows the IR spectra acquired during the CO TPD experiment on CoO_x/ZrO_2. In Fig. 8a, the broad band from 3600 to 3000 cm^{-1} is again due to the OH vibration mode of physisorbed H_2O. Following CO adsorption, the three negative bands due to CO interaction with surface hydroxyls were far less intense on the CoO_x/ZrO_2 catalyst as compared to ZrO_2. The bands at 2969 and 2864 cm^{-1} from bidentate formate [38] are present but weaker than were observed on ZrO_2. The bands at 2360 and 2345 cm^{-1} are due to CO_2. The low wavenumber region shown in Fig. 8b reveals several types of carbonate species that where also observed on ZrO_2. The bands at 1633 cm^{-1} and 1360 cm^{-1} have been assigned to bidentate bicarbonate [39,43]. As was observed on the ZrO_2, the bidentate bicarbonate bands red shift and decrease in intensity as the carbonate band at 1558 cm^{-1} grows with increasing temperature. The band at 1577 cm^{-1} is assigned to bidentate formate [38] and 1558 cm^{-1} is again attributed to surface carbonate species [43].

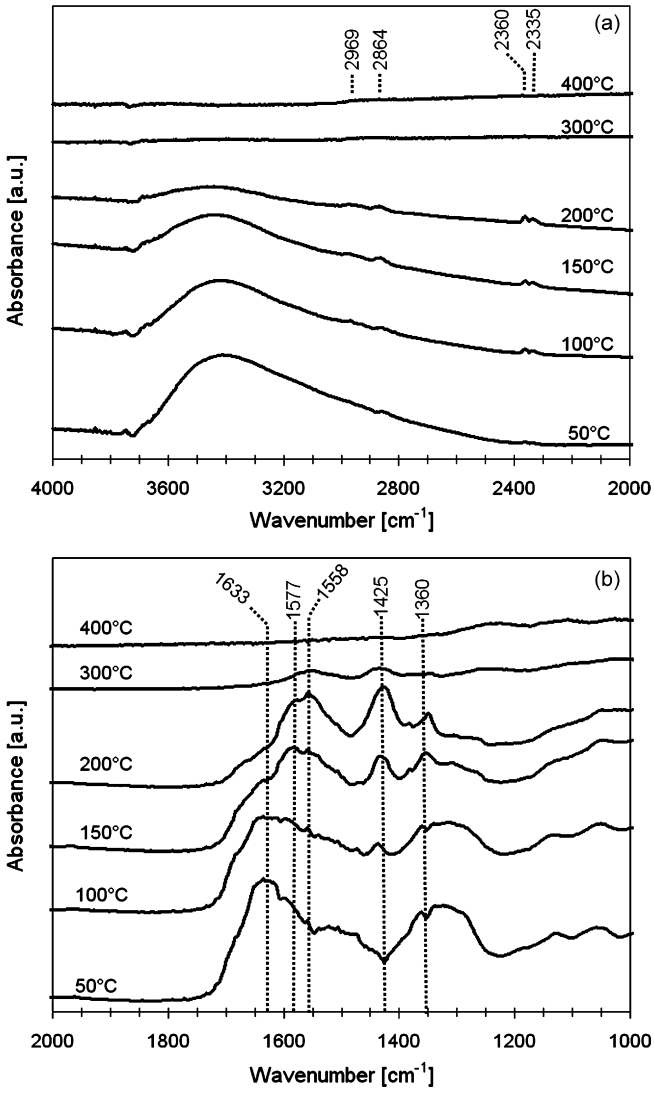

Fig. 8. DRIFTS spectra of CoO_x/ZrO_2 under 25 cm^3/min He following 30 min adsorption of 1% CO, referenced to CoO_x/ZrO_2 under He flow at each temperature.

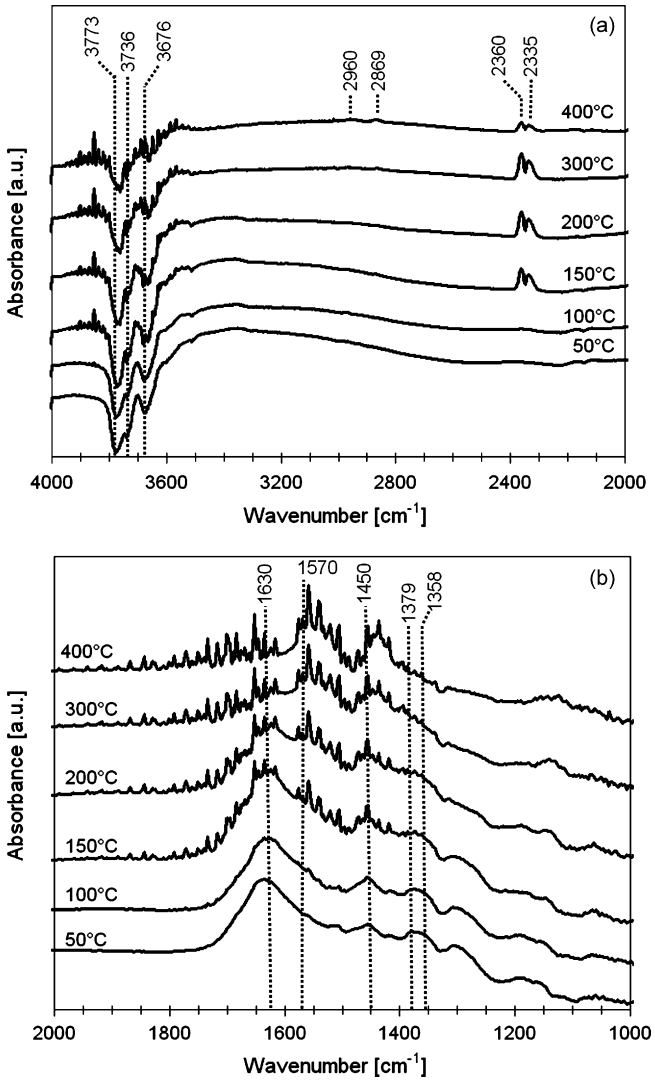

Fig. 9. *In situ* DRIFTS spectra of ZrO_2 under 25 cm^3/min of PROX gas (1% CO, 1% O_2, 60% H_2, balance He) referenced to ZrO_2 under He flow at each temperature.

Bidentate formate bands at 1379 cm^{-1} and 1358 cm^{-1} are difficult to resolve due to the broad feature centered at 1360 cm^{-1}. The 1438 cm^{-1} band due to ionic carbonate grows with temperature and red shifts to 1425 cm^{-1} by 200 °C [39] before disappearing at higher temperatures. This band was significantly stronger on CoO_x/ZrO_2 as opposed to ZrO_2. In comparison to the TPD on ZrO_2, the surface species are more easily desorbed on CoO_x/ZrO_2. By 300 °C, all the surface species have essentially desorbed as indicated by the absence of absorbance bands at 300 °C and 400 °C, whereas surface species were still observed at 400 °C on ZrO_2.

3.5.2. *In situ PROX*

The surface species on ZrO_2 and CoO_x/ZrO_2 under reaction conditions were examined using in situ DRIFTS to monitor the sample under CO, O_2, and H_2 flow. Fig. 9 shows the spectra during the in situ PROX reaction on ZrO_2. The terminal, bi-bridged, and tri-bridged hydroxyl groups are again observed at 3773, 3736, and 3676 cm^{-1}, respectively. Under reaction conditions, these hydroxyl groups are present even at 400 °C. The broad band from 3600 to 3000 cm^{-1} due to physisorbed water decreases with increasing temperature. The gas phase CO_2 bands at 2360 cm^{-1} and 2335 cm^{-1} indicate that significant CO oxidation occurs over ZrO_2 at 150 °C at above. Bands at 2170 cm^{-1} and 2116 cm^{-1} due to gas phase CO were clearly observed and decreased with intensity as the CO_2 band intensities increased. In the low wavenumber region, surface species similar to those observed during the CO TPD are present. Bidentate bicarbonate (1630 cm^{-1}), formate (2960, 2869, 1570, 1379, and 1358 cm^{-1}), and ionic carbonate (1450 cm^{-1}) bands are again observed. As the reaction temperature increases, the bidentate bicarbonate band decreases in intensity while formate bands increase in intensity. The ionic carbonate increases in intensity and undergoes a red shift to 1435 cm^{-1}. The rotational bands due to gas phase water created from H_2 combustion at 150 °C and above, however, decrease our ability to resolve band contributions at high temperatures.

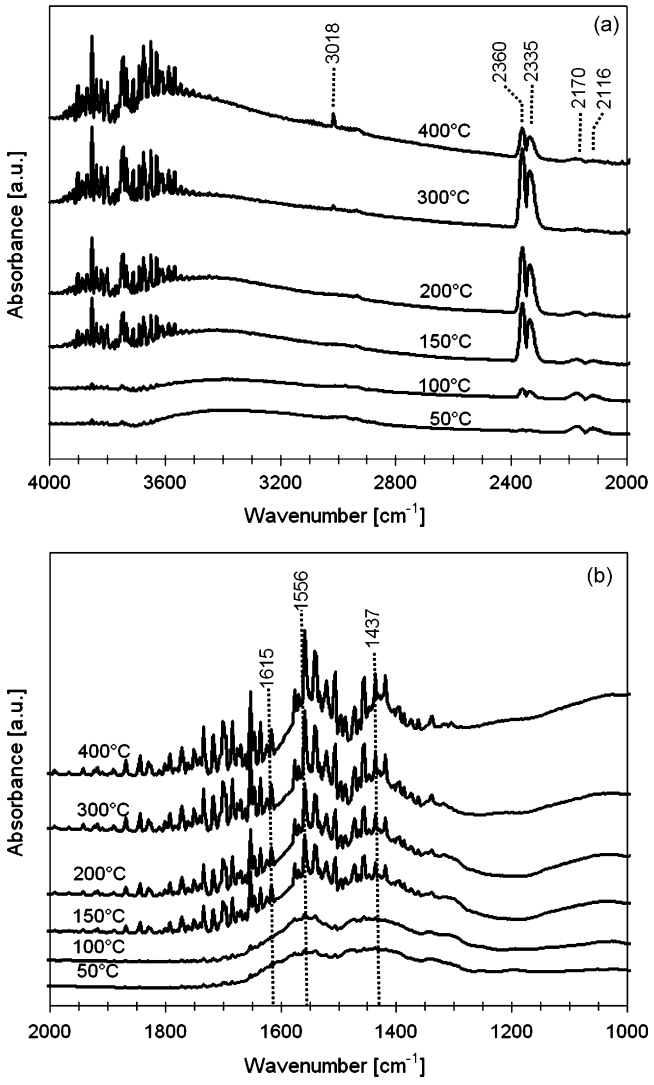

Fig. 10. *In situ* DRIFTS spectra of CoO_x/ZrO_2 under 25 cm^3/min of PROX gas (1% CO, 1% O_2, 60% H_2, balance He) referenced to CoO_x/ZrO_2 under He flow at each temperature.

Fig. 10 shows the *in situ* PROX reaction on CoO_x/ZrO_2. The broad band from 3600 to 3000 cm^{-1} from physisorbed water is again present. Gas phase CO_2 (2360 and 2335 cm^{-1}) is clearly observed at 100 °C and higher. Bands intensities from gas phase CO (2170 and 2116 cm^{-1}) were observed to decrease as the CO_2 band intensities increased. At 300 °C a band at 3018 cm^{-1} from gas phase CH_4 is observed. This band grows in intensity as the temperature is raised to 400 °C. The intensity of the CO_2 bands also decreases as temperature is increased from 300 °C to 400 °C. These findings are consistent with the temperature-programmed reaction study, which indicated that methanation occurred at 300 °C at the expense of CO oxidation. The onset of methanation and decline in CO oxidation activity can be attributed to a partial reduction of cobalt oxide at elevated temperatures in excess H_2 [30]. The PROX reaction conditions over CoO_x/ZrO_2 give rise to similar carbonate species as were observed during the CO TPD in the low wavenumber region. Bidentate bicarbonate at 1615 cm^{-1} is present at low temperatures and decreases in intensity with increasing temperature. The carbonate feature at 1556 cm^{-1} and ionic carbonate band at 1437 cm^{-1} increase in intensity with increasing temperature. In contrast to the CO TPD on CoO_x/ZrO_2, the formate bands are not be readily observed under reaction conditions, although minor contributions could be masked in broad carbonate features. At 150 °C and higher temperatures, the rotational bands of water are observed due to H_2 combustion and create difficulty in making precise assignments.

4. Conclusions

A CoO_x/ZrO_2 catalyst was tested for the preferential oxidation of CO under various conditions and showed both high activity for CO oxidation and O_2 selectivity to CO_2. Increasing GHSV was observed to cause a decrease in CO conversion and an increase in O_2 selectivity to CO_2. Experiments adjusting the CO/O_2 ratio showed an increase in this ratio led to lower CO conversion but higher O_2 selectivity to CO_2. Following CO adsorption, DRIFTS studies showed formate and carbonate species on both ZrO_2 and CoO_x/ZrO_2, and these species were more readily desorbed on CoO_x/ZrO_2. Negative bands corresponding to CO interaction with hydroxyls were observed on ZrO_2 during both CO TPD and *in situ* PROX experiments. During reaction conditions on CoO_x/ZrO_2, carbonate species were observed but formate species could not be detected. The oxidation of CO to CO_2 could also be observed at 100 °C and higher temperatures, while at 300 °C and 400 °C methanation occurred and the intensity of CO_2 absorbance bands decreased. Time-on-stream reaction studies showed that the catalyst lost some of its initial activity when operated at 175 °C which is attributed to the partial reduction of cobalt oxide, as shown by TPR studies in which the catalyst underwent pretreatment in H_2 at various temperatures. The partial reduction of cobalt oxide could also lead to the formation of methane under PROX conditions and was observed by temperature-programmed reaction and *in situ* DRIFTS over CoO_x/ZrO_2.

Acknowledgements

The financial support provided for this work by the Ohio Coal Development Office and the Ohio Department of Development through a Wright Center of Innovation is gratefully acknowledged. The authors would also like to acknowledge NSF support for acquisition of the XPS system under NSF-DMR grant #0114098.

References

[1] B.C.H. Steele, A. Heinzel, Nature 414 (2001) 345.
[2] A. Ghenciu, Curr. Opin. Solid St. Mat. Sci. 6 (2002) 389.
[3] D.J. Suh, C. Kwak, J.-H. Kim, S.M. Kwon, T.-J. Park, J. Power Sources 142 (2005) 70.
[4] C. Kwak, T.-J. Park, D.J. Suh, Chem. Eng. Sci 5 (2005) 1211.
[5] F. Marino, C. Descorme, D. Duprez, Appl. Catal. B 54 (2004) 59.
[6] T. Ince, G. Uysal, A. Akin, R. Yildirim, Appl. Catal. A 292 (2005) 171.
[7] G. Uysal, N. Akin, I. Oensan, R. Yildirim, Catal. Lett. 108 (2006) 193.
[8] P. Ratnasamy, D. Srinivas, C.V.V. Satyanarayana, P. Manikandan, R. Kumaran, S. Senthil, M. Sachin, V.N. Shetti, J. Catal. 212 (2004) 455.

[9] D.L. Trimm, Z.I. Onsan, Catal. Rev. Sci. Eng. 43 (2001) 31.
[10] J.R. Ladebeck, J.P. Wagner, Handbook of Fuel Cells—Fundamentals, Technology and Applications, vol. 3, Wiley & Sons, 2003, pp. 190-201, ISBN: 0-471-49926-9.
[11] J. Ayastuy, M. Gutierrez-Ortiz, J. Gonzalez-Marcos, A. Aranzabal, J. Gonzalez-Velasco, Ind. Eng. Chem. Res. 44 (2005) 41.
[12] R. Ahluwalia, Q. Zhang, D. Chmielewski, K. Lauzze, M. Inbody, Catal. Today 99 (2005) 271.
[13] S.H. Oh, R.M. Sinkevitch, J. Catal. 142 (1993) 254.
[14] A. Wootsch, C. Descorme, D. Duprez, J. Catal. 225 (2004) 259.
[15] A.K. Sinha, S. Seelan, M. Okumura, T. Akita, S. Tsubota, M. Haruta, J. Phys. Chem. B 109 (2005) 3956.
[16] I. Rosso, C. Galletti, G. Saracco, E. Garrone, V. Specchia, Appl. Catal. B 48 (2004) 195.
[17] M. Shou, K. Tanaka, K. Yoshioka, Y. Moro-oka, S. Nagano, Catal. Today 90 (2004) 255.
[18] M. Haruta, S. Tsubota, T. Kobayashi, H. Kageyama, M.J. Genet, B. Delmon, J. Catal. 144 (1993) 175.
[19] M.J. Kahlich, H.A. Gasteiger, R.J. Behm, J. Catal. 182 (1999) 430.
[20] S.S. Pansare, A. Sirijaruphan, J.G. Goodwin Jr., J. Catal. 234 (2005) 151.
[21] C. Rossignol, S. Arrii, F. Morfin, L. Piccolo, V. Caps, J. Rousset, J. Catal. 203 (2005) 476.
[22] B. Atalik, D. Uner, J. Catal. 241 (2006) 268.
[23] C. Wang, C. Tang, H. Tsai, M. Kuo, S. Chien, Catal. Lett. 107 (2006) 31.
[24] F. Gracia, W. Li, E. Wolf, Catal. Lett. 91 (2003) 235.
[25] B. Chang, Y. Lu, B. Tatarchuk, Chem. Eng. J. 115 (2006) 195.
[26] G. Roberts, P. Chin, X. Sun, J. Spivey, Appl. Catal. B Environ. 46 (2003) 601.
[27] M. Watanabe, H. Uchida, K. Ohkubo, H. Igarashi, Appl. Catal. B 46 (2003) 595.
[28] K. Omata, Y. Kobayashi, M. Yamada, Catal. Commun. 6 (2005) 563.
[29] S. Özkara, A. Akin, Z. Misirli, A. Aksoylu, Turkish J. Chem. 29 (2005) 219.
[30] Y. Teng, H. Sakurai, A. Ueda, T. Kobayashi, Int. J. Hydrogen Energy 24 (1999) 355.
[31] E.M. Holmgreen, M.M. Yung, U.S. Ozkan, Appl. Catal. B 74 (2007) 73.
[32] M.M. Yung, E.M. Holmgreen, U.S. Ozkan, J. Catal. 247 (2007) 356.
[33] M.M. Yung, E.M. Holmgreen, U.S. Ozkan, Catal. Lett. 118 (2007) 180–186.
[34] P.A. Chernavskii, A.S. Lermontov, G.V. Pankina, S.N. Torbin, V.V. Lunin, Kinet. Catal. 43 (2002) 292.
[35] S. Sun, K. Tsubaki, K. Fujimoto, Appl. Catal. A 202 (2000) 121.
[36] M.J. Tiernan, E.A. Fesenko, P.A. Barnes, G.M.B. Parkes, M. Ronane, Thermochim. Acta 379 (2001) 163.
[37] K.T. Jung, A.T. Bell, J. Catal. 204 (2001) 339.
[38] H. Kalies, N. Pinto, G.M. Pajonk, D. Bianchi, Appl. Catal. A 202 (2000) 197.
[39] I.A. Fisher, A.T. Bell, J. Catal. 172 (1997) 222.
[40] D. Bianchi, T. Chafik, M. Khalfallah, S.J. Teichner, Appl. Catal. A 105 (1993) 223.
[41] Y. Kohno, T. Tanaka, T. Funabiki, S. Yoshida, J. Chem Soc. Faraday Trans. 94 (1998) 1875.
[42] Z.-Y. Ma, C. Yang, W. Wei, W.-H. Li, Y.-H. Sun, J. Mol. Catal. A 231 (2005) 75.
[43] K.D. Dobson, A.J. McQuillan, Langmuir 13 (1997) 3392.